
ProstaTD: A Large-scale Multi-source Dataset for Structured Surgical Triplet Detection

Yiliang Chen¹, Zhixi Li², Cheng Xu¹, Alex Qinyang Liu³,
Xuemiao Xu⁴, Jeremy Yuen-Chun Teoh³, Shengfeng He⁵, Jing Qin¹

¹School of Nursing, The Hong Kong Polytechnic University

²Nanfang Hospital, Southern Medical University

³Department of Surgery, The Chinese University of Hong Kong

⁴South China University of Technology, ⁵Singapore Management University

Abstract

Surgical triplet detection has emerged as a pivotal task in surgical video analysis, with significant implications for performance assessment and the training of novice surgeons. However, existing datasets such as CholecT50 exhibit critical limitations: they lack precise spatial bounding box annotations, provide inconsistent and clinically ungrounded temporal labels, and rely on a single data source, which limits model generalizability. To address these shortcomings, we introduce **ProstaTD**, a large-scale, multi-institutional dataset for surgical triplet detection, developed from the technically demanding domain of robot-assisted prostatectomy. ProstaTD offers clinically defined temporal boundaries and high-precision bounding box annotations for each structured triplet action. The dataset comprises 60,529 video frames and 165,567 annotated triplet instances, collected from 21 surgeries performed across multiple institutions, reflecting a broad range of surgical practices and intraoperative conditions. The annotation process was conducted under rigorous medical supervision and involved more than 50 contributors, including practicing surgeons and medically trained annotators, through multiple iterative phases of labeling and verification. ProstaTD is the largest and most diverse surgical triplet dataset to date, providing a robust foundation for fair benchmarking, the development of reliable surgical AI systems, and scalable tools for procedural training. The dataset and code are available at Github.

1 Introduction

Surgical triplet recognition is a fundamental task in surgical data science. It involves identifying <instrument, verb, target> triplets, which represent the tool in use, the action performed, and the anatomical target, from each frame of surgical videos. This task supports the development of context-aware decision support systems and contributes to improved surgical safety, procedural standardization, and operational efficiency [1–3].

The field was initiated with the release of CholecT40 [4], the first benchmark for surgical triplet recognition in laparoscopic cholecystectomy. It provided frame-level triplet class labels for training models and was later extended through CholecT45 [5] and CholecT50 [6], which included 5 and 10 additional surgical videos, respectively. Currently, CholecT50 is the most widely adopted dataset for this task [7–9]. While CholecTriplet 2022 Challenge [10] advanced the field by framing surgical triplet detection as a task involving both recognition and spatial localization, it relied primarily on weak supervision using frame-level triplet class labels, limiting the precision of spatial localization.

Despite these contributions, CholecT50 [6] has three critical limitations:

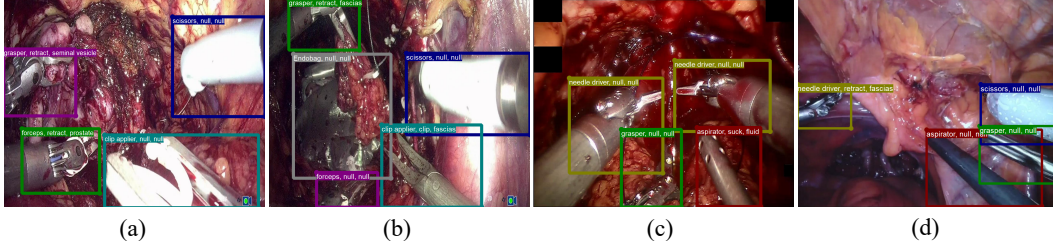


Figure 1: **Examples of labeled surgical triplets in our ProstaTD dataset.** ProstaTD offers clinically defined temporal boundaries and high-precision bounding box annotations for each structured triplet action, curated from diverse, multi-institutional surgical sources, establishing a strong foundation for precise and robust triplet detection. Here, (a) and (b) are examples from our in-house collected videos at PWH, (c) from the PSI-AVA dataset [11], and (d) from the ESAD dataset [12]. *All videos were comprehensively annotated by our team.*

1. **No bounding box annotations:** CholecT50 provides only class labels, without spatial localization. This restricts the task to weakly supervised settings and limits localization accuracy.
2. **Unclear and inconsistent temporal boundaries:** The dataset lacks clear guidelines on when an action should start or end. It is ambiguous whether annotation should begin when the instrument enters the field of view or only when it contacts the anatomical target, and whether it should end upon disengagement or upon exit. This uncertainty leads to inconsistent labeling and undermines the model’s ability to learn temporal dynamics and tool-target interactions.
3. **Lack of diversity in data sources:** CholecT50 originates from a single institution, offering limited variability in surgical practices and instruments. In practice, instruments of the same type may differ significantly between manufacturers, and surgical strategies such as instrument pairing often vary between hospitals. Consequently, models trained on CholecT50 struggle to generalize to real-world clinical environments.

To address these limitations, we introduce **ProstaTD**, the first large-scale surgical triplet detection dataset encompassing full-length surgical procedures with precise multi-instrument localization. ProstaTD enables simultaneous and reliable recognition and localization of surgical triplets, a capability essential for modeling tool-tissue interactions and developing intelligent systems for intraoperative guidance. The dataset includes 21 robot-assisted prostatectomy videos, totaling 60,529 annotated frames and 165,567 surgical triplet instances. These were sourced from three heterogeneous domains: 4 videos from the publicly available ESAD [12], 8 from PSI-AVA [11] dataset, and 9 newly acquired from the Prince of Wales Hospital in Hong Kong. Compared to existing cholecystectomy datasets, ProstaTD offers higher instrument concurrency, greater anatomical complexity, and increased domain diversity. These characteristics better reflect the variability and challenges of real-world high-complexity surgical environments. Each frame in ProstaTD is annotated with structured triplet information, including precise bounding boxes for all visible instruments, detailed action (verb) labels, and anatomical target identifiers. All annotations are constrained within expert-defined temporal boundaries curated by experienced urologists, ensuring both clinical accuracy and temporal consistency. Fig. 1 showcases representative examples of the annotated triplets in ProstaTD.

We conduct extensive evaluations using baseline and state-of-the-art models. Results show that the fine-grained spatial annotations in ProstaTD significantly improve model performance in both localization precision and triplet recognition robustness. ProstaTD thus provides a comprehensive foundation for advancing surgical video analysis, facilitating model development, supporting clinical decision-making, and enhancing procedural training.

In summary, our contributions are threefold:

- We present the first large-scale, multi-source dataset for surgical triplet detection and tracking in full-length procedures beyond cholecystectomy. It captures complex surgical scenarios with diverse instrument types, anatomical contexts, and institutional practices, providing a robust foundation for developing generalizable and high-performing models.
- We establish clinically grounded, standardized criteria for defining action boundaries, reducing annotation ambiguity and promoting temporal consistency.
- We provide dense frame-level annotations, including precise instrument bounding boxes and clinically validated triplet labels, facilitating fine-grained spatial reasoning in model development.

Table 1: Comparison of existing surgical datasets with our ProstaTD, highlighting the unique attributes required for surgical triplet detection. LC and RARP denote laparoscopic cholecystectomy and robot-assisted radical prostatectomy, respectively. Full BBox indicates that every frame is fully annotated with precise bounding boxes.

Dataset	Task	Attributes					Statistics	
		Supervised Triplet Detect	Full BBox	Triplet Action Boundary	Multiple Sources	Complete Surgery	No. Instances	No. Triplets
Cholec80-locations [16]	LC		✓			✓	6,471	–
CholecTrack20 [17]	LC		✓			✓	65,200	–
ESAD [12]	RARP		✓			✓	46,753	–
PSI-AVA [11]	RARP					✓	5,804	–
CholecQ [18]	LC	✓	✓				14,480	17
CholecT45 [5]	LC					✓	146,394	100
CholecT50 [6]	LC					✓	161,988	100
ProstaTD (Ours)	RARP	✓	✓	✓	✓	✓	165,567	89

2 Related Work

Public Prostatectomy Datasets. Several prostatectomy datasets have been introduced in recent years, including GraSP [13], TAPIS [14], PSI-AVA [11], and SAR-RARP50 [15]. These were developed for varied downstream tasks such as phase segmentation or instrument tracking and contain partially overlapping surgical videos. The ESAD dataset [12], released for the SARAS-ESAD2021 challenge [12], focuses on surgical action recognition. However, as summarized in Table 1, none of these datasets support surgical triplet detection, which requires explicit annotation of instrument, action, and target interactions. For example, PSI-AVA includes labels for instruments and actions but omits target annotations, limiting its suitability for comprehensive triplet-level analysis. To bridge this gap, we augmented our dataset with surgical triplet annotations in four ESAD and eight PSI-AVA videos. This integration results in a more complete and task-specific dataset tailored for modeling fine-grained instrument-action-target dynamics in prostatectomy procedures.

Surgical Triplet Datasets. While many surgical video datasets have emerged, most are not designed to support triplet-based reasoning. Datasets such as Cholec80-locations [16] and CholecTrack20 [17] provide bounding box annotations but focus primarily on instrument tracking, without structured action-target associations required for triplet detection.

A few datasets offer partial triplet-style annotations but are limited in scope, accessibility, or domain relevance. For instance, MISAW [19] is restricted to simulated anastomosis tasks. RLLS-I2M [20], Cataract [21], and PhacoQ [22] are not publicly available, making comparative analysis infeasible. CholecQ [22] is a notable exception, offering bounding box annotations for triplet-like structures. However, it is constrained to 3-second clips from Cholec80 [23], resulting in high frame redundancy and limited temporal diversity. It lacks full-procedure coverage and contains only 17 unique triplet types, far fewer than the 100 in CholecT50 [6] or the 89 in our proposed **ProstaTD**. These limitations render CholecQ a toy-scale dataset inadequate for robust, real-world triplet modeling (see Table 1).

The CholecTriplet series, starting from CholecT40 [4] and later extended to CholecT45 [5] and CholecT50 [6], represents the most comprehensive existing effort for surgical triplet recognition. CholecT50 includes 161,988 annotated triplet instances across 100 classes. However, it only provides class labels at the frame level, lacking spatial bounding boxes and standardized temporal boundaries for surgical actions. Furthermore, it is limited to a single institution, which restricts its generalizability to more diverse and complex surgical scenarios.

The proposed ProstaTD addresses the above limitations and is specifically designed for surgical triplet detection in high-complexity procedures. It features dense spatial annotations, clinically standardized action boundaries, and multi-institutional data sources. These attributes enable precise triplet localization, consistent temporal labeling, and broad generalizability, supporting a more robust and structured analysis of surgical videos.

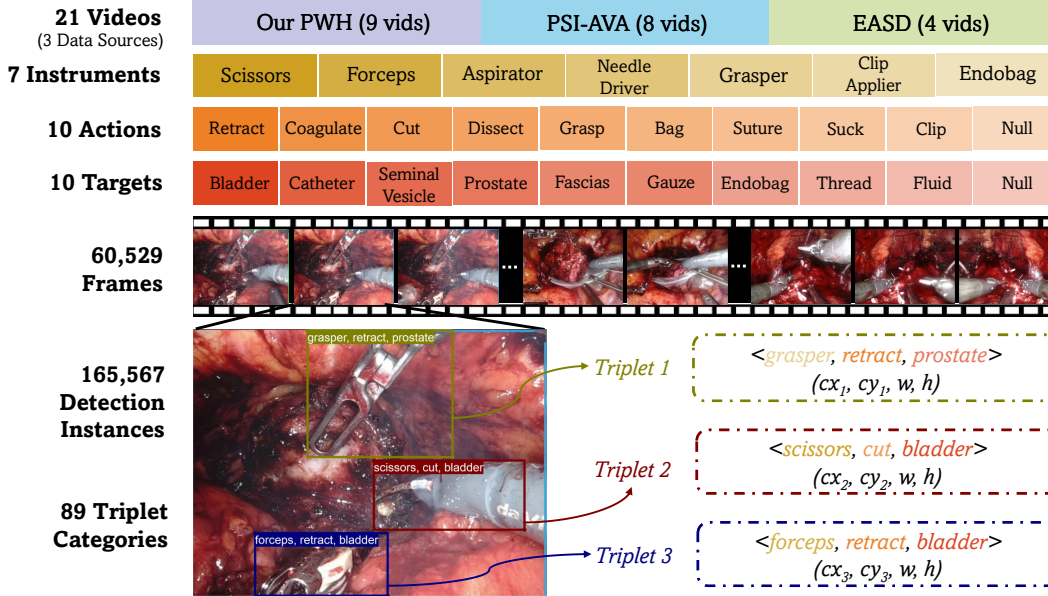


Figure 2: **Overview of the ProstaTD dataset structure.** The dataset consists of 21 videos curated from three sources: our in-house collection at PWH, PSI-AVA [11], and EASD [12]. *All videos were comprehensively annotated by our team, covering 7 instruments, 10 actions, and 10 targets.* In total, the dataset contains 60,529 frames, 165,567 annotated instances, and 89 unique surgical triplet categories, with each frame exhaustively labeled using precise bounding boxes.

3 ProstaTD Dataset

3.1 Problem Definition of Surgical Triplet Detection

Given a video dataset $V = \{V_1, V_2, \dots, V_n\}$ of laparoscopic surgeries, each video V_i consists of a temporally ordered frame sequence $F = \{F_1, F_2, \dots, F_m\}$. Each frame F_t may contain multiple instrument instances, each annotated with a bounding box $B = \{(c_x, c_y, w, h)\}$, where (c_x, c_y) denotes the center coordinates, and w and h represent the width and height, respectively. In addition, every instance is assigned with a triplet class label $C \in \{C_1, C_2, \dots, C_N\}$, where C_i corresponds to a predefined combination of an instrument, an action, and a target. Here, N denotes the total number of possible triplet combinations, which is determined by the surgical task. The goal of surgical triplet detection is to identify all valid triplets $\mathcal{T}_t = \{C_1, C_2, \dots, C_k\}$ within each frame F_t , enabling precise detection and classification of all instrument-action-target interactions.

3.2 Data Collection

Our dataset, illustrated in Fig. 2, integrates three sources: our in-house surgical videos collected from PWH, the publicly available PSI-AVA dataset [11] and the ESAD dataset [12]. Here, ESAD is released under the CC-BY-NC-SA-4.0 license and PSI-AVA is hosted by MIT. The PWH videos were recorded with institutional ethical approval, and the final release of our dataset will also comply with the CC-BY-NC-SA-4.0 license. Notably, we did not utilize any existing annotations from ESAD or PSI-AVA, even when they were partially relevant to our task. This decision was driven by differences in data sources and the need for a unified annotation protocol to ensure consistent labeling of surgical actions, targets, and bounding boxes. Accordingly, guided by the expert insights of our team’s urologist, we developed and strictly followed our own annotation criteria throughout the process.

3.3 Annotation Design

Categories Design. As shown in Fig. 2, our annotations schema comprises 7 surgical instruments, 10 actions, and 10 targets. These categories were determined through consensus among ten professional surgeons, with some labels merged to ensure consistency and reduce redundancy. For example,

“scissors” and “monopolar scissors” were unified under the label “scissors”, while “prograsp” and another type of “grasper” were merged into a single “grasper” category. For surgical instrument bounding boxes, we adopted a consistent strategy: for instruments with well-defined contours, only the head and joint regions were enclosed, whereas instruments with indistinct boundaries, such as “aspirator”, were annotated using full-enclosure bounding boxes. These annotation rules were consistently applied across all instrument categories. Following the practice of CholecT50 [6], rare categories were merged with semantically similar labels based on clinical relevance, as agreed upon by professional surgeons. In ambiguous scenarios, such as excising prostate regions situated between two anatomical targets, the determination of the correct target was delegated to the five most senior surgeons on our team. These cases were resolved via a majority vote. Detailed merging rules and bounding box annotation protocols for each category are provided in the supplementary materials.

Temporal Boundaries of Triplet Actions. Unlike CholecT50 [6], we established unified guidelines to define the temporal boundaries of surgical triplet actions. Importantly, actions were not annotated based solely on the presence of a surgical tool in the frame, as such an approach resembles instance-level step recognition and lacks alignment with clinical assessment of surgical skill. Following collaborative discussions, actions were categorized into two types: continuous actions and momentary actions. For continuous actions, such as lymph node dissection along the iliac vessels over multiple frames, the action was defined to start only when the tool makes contact with or is extremely close to, the target. The action was deemed to end when the tool departed from the same target for more than 2 seconds. For momentary actions, such as cutting sutures with scissors, the temporal window was defined with more flexibility: annotations included up to 2 seconds before and after the moment of tool-target contact. This clinically informed strategy ensures temporally precise and semantically meaningful annotation of triplet actions, better aligning with real-world surgical practices.

Data Format. For every frame we save a label file (*.txt*) in the `labels/` folder. Each file contains one row *per detected triplet* in the form $\langle tri, i, a, t, c_x, c_y, w, h \rangle$, where *tri*, *i*, *a*, *t* are the triplet, instrument, action, and target IDs, and (c_x, c_y, w, h) denote the bounding-box centre, width, and height (see Fig. 2), respectively. Files are named $\langle videoname_frameid \rangle.txt$; and the corresponding image is stored in `images/` as $\langle videoname_frameid \rangle.jpg$. The directory layout follows the YOLO convention, but each label row prepends the four IDs (*tri*, *i*, *a*, *t*) to the standard box parameters.

3.4 Annotation Process

Labeling Tools. During the annotation process, we employed two primary tools: a customized version of LabelMe¹ and a purpose-built tool specifically developed for annotating triplet action and targets. The first tool, modified on LabelMe, is used for annotating the bounding boxes and assigning instrument categories. It also includes features for visualizing and editing triplet annotations on a per-frame basis. Examples of such annotated images are illustrated in Fig. 1. The second tool, named LabelTri, is a dedicated interface designed for batch labeling actions and targets within triplets. Given that instrument categories and bounding box coordinates were already defined, this tool enables annotators to assign action and target labels to specified instruments across a defined temporal range, indicated by the start `frameid` and end `frameid`. This design leverages the temporal continuity commonly observed in surgical actions. Both software will be made publicly available.

Semi-Automatic Annotation for Surgical Instruments. In the initial phase of annotation, we focused on labeling the types and bounding boxes of surgical instruments used in prostatectomy procedures. To support this task, we recruited 43 additional part-time student assistants, resulting in a total of 48 annotators. Among them, 20 students with medical backgrounds were assigned to conduct multiple rounds of review and quality control. Initial annotations were generated based on pre-labeled results from our previously developed cystoscopic surgical instrument detection model. Although bladder and prostate surgeries share visual similarities, domain-specific differences require extensive manual refinement. Consequently, our team performed at least three rounds of manual corrections on selected videos before using them to fine-tune the instrument detection model for subsequent annotation generation. After five iterative cycles of this semi-automatic training and correction process, we successfully completed both instrument type classification and bounding box annotations for all surgical instruments across the entire video dataset.

¹<https://labelme.io/>

Table 2: Percentage distribution of triplet instances per frame in surgical triplet datasets between CholecT50 [6] and our ProstaTD. Values are in %.

Dataset	0	1	2	3	4	5	6	7
CholecT50 [6]	10.970	35.180	47.100	6.750	0.000	0.000	0.000	0.000
ProstaTD	0.476	6.592	34.322	38.925	17.122	2.344	0.216	0.002

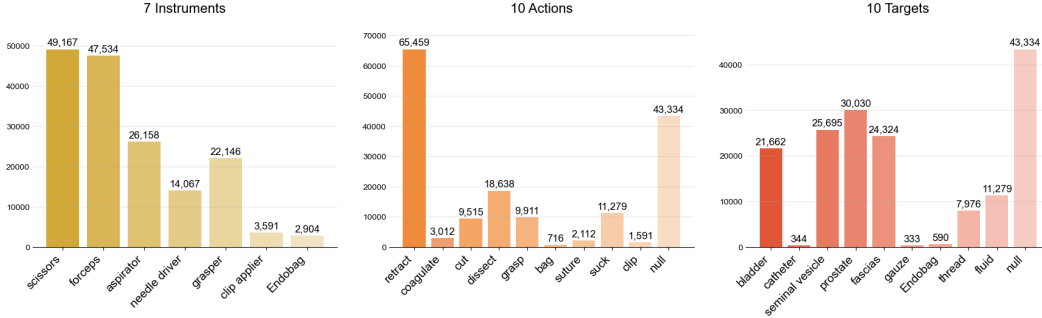


Figure 3: Statistics of component labels in ProstaTD, showing the distributions of instruments (left), actions (center), and targets (right). The label counts indicate the frequency of each component, highlighting the dataset’s diversity and task complexity.

Surgical Action and Target Labeling. In the second phase, we enriched the instrument annotations from the first phase by assigning corresponding actions and targets. Unlike the first phase, which could be carried out by student annotators, this stage required substantial medical expertise. Although we employed the batch annotation tool, LabelTri, the annotation and refinement process were considerably more time-consuming. This phase was conducted by ten surgeons and fourteen senior students with strong medical backgrounds. To ensure label accuracy, each frame was reviewed and corrected by at least three team members. This process resulted in a high-quality ProstaTD dataset comprising 89 triplet categories and 165,567 annotated instances, as illustrated in Fig. 2.

4 Analysis of the ProstaTD Dataset

4.1 Complexity Analysis of ProstaTD

According to the Hospital Authority of Hong Kong², cholecystectomy is classified as a major procedure in Hong Kong, whereas prostatectomy is designated as ultra-major, reflecting a higher level of surgical complexity. This distinction highlights the increased technical demands and environmental intricacy associated with prostatectomy procedures. The complexity gap is quantitatively reflected in Table 2, which compares the distribution of concurrent triplet instances in CholecT50 (cholecystectomy) and our proposed ProstaTD (prostatectomy) datasets.

ProstaTD exhibits substantially more complex surgical scenes compared to CholecT50 [6]. In CholecT50, the majority of frames contain only one or two triplet instances (35.18% and 47.10%, respectively), with no frames exceeding three instances. In contrast, our ProstaTD demonstrates a broader distribution: 38.93% of frames contain three instances, 17.12% contain four, and a non-negligible proportion contains six or more. This distribution underscores the inherent complexity of prostatectomy surgeries, where multiple instruments often operate concurrently within a confined anatomical space. Furthermore, the increased instrument count frequently results in overlapping instances, and the anatomically intricate structures surrounding the prostate introduce additional visual complexity. Together, these factors pose significant challenges for triplet detection models, emphasizing the need for datasets like ProstaTD that capture the full scope of surgical difficulty.

4.2 Distribution of Triplet Component

The prostatectomy procedure can be broadly divided into two main phases: the dissection phase and the anastomosis phase. As the dissection phase comprises the majority of the operation, instruments such as monopolar scissors and bipolar forceps, which are primarily used during this phase, exhibit the

²<https://www3.ha.org.hk/fnc/operations.aspx?lang=ENG>

Table 3: Frequency of triplet occurrences. Here, “driver” refers to **needle driver**, “applier” to **clip applier**, and “vesicle” to **seminal vesicle**.

Triplet	Count	Triplet	Count	Triplet	Count
scissors,retract,bladder	661	scissors,retract,catheter	102	scissors,retract,vesicle	1175
scissors,retract,prostate	1750	scissors,retract,fascias	1077	scissors,retract,gauze	90
scissors,retract,Endobag	101	scissors,coagulate,bladder	105	scissors,coagulate,vesicle	101
scissors,coagulate,prostate	43	scissors,coagulate,fascias	214	scissors,cut,bladder	3306
scissors,cut,catheter	4	scissors,cut,vesicle	632	scissors,cut,prostate	5032
scissors,cut,fascias	489	scissors,cut,thread	54	scissors,dissect,bladder	621
scissors,dissect,vesicle	5789	scissors,dissect,prostate	5039	scissors,dissect,fascias	6935
scissors,null,null	15849	forceps,retract,bladder	6652	forceps,retract,catheter	30
forceps,retract,vesicle	8206	forceps,retract,prostate	8906	forceps,retract,fascias	8086
forceps,retract,Endobag	68	forceps,coagulate,bladder	489	forceps,coagulate,vesicle	515
forceps,coagulate,prostate	1003	forceps,coagulate,fascias	542	forceps,dissect,vesicle	29
forceps,dissect,prostate	45	forceps,dissect,fascias	180	forceps,grasp,catheter	29
forceps,grasp,vesicle	63	forceps,grasp,prostate	28	forceps,grasp,fascias	446
forceps,grasp,gauze	130	forceps,grasp,Endobag	100	forceps,grasp,thread	1013
forceps,suture,bladder	69	forceps,suture,prostate	33	forceps,suture,fascias	15
forceps,null,null	10857	aspirator,retract,bladder	6379	aspirator,retract,catheter	4
aspirator,retract,vesicle	900	aspirator,retract,prostate	1349	aspirator,retract,fascias	2893
aspirator,retract,Endobag	13	aspirator,suck,fluid	11279	aspirator,null,null	3341
driver,retract,bladder	830	driver,retract,prostate	10	driver,retract,fascias	277
driver,grasp,bladder	18	driver,grasp,catheter	29	driver,grasp,fascias	14
driver,grasp,gauze	79	driver,grasp,Endobag	4	driver,grasp,thread	6821
driver,suture,bladder	1690	driver,suture,prostate	248	driver,suture,fascias	57
driver,null,null	3990	grasper,retract,bladder	699	grasper,retract,catheter	55
grasper,retract,vesicle	7894	grasper,retract,prostate	5069	grasper,retract,fascias	2183
grasper,grasp,catheter	93	grasper,grasp,vesicle	25	grasper,grasp,prostate	289
grasper,grasp,fascias	330	grasper,grasp,gauze	34	grasper,grasp,Endobag	278
grasper,grasp,thread	88	grasper,null,null	5109	applier,clip,bladder	143
applier,clip,vesicle	366	applier,clip,prostate	630	applier,clip,fascias	426
applier,clip,Endobag	26	applier,null,null	2000	Endobag,bag,prostate	556
Endobag,bag,fascias	160	Endobag,null,null	2188	Total:	165567

highest usage frequency. In contrast, needle drivers are predominantly utilized during the anastomosis phase. Aspirators and graspers are commonly employed in both phases: aspirators are used for smoke and blood suction, while graspers assist with organ retraction and exposure. Meanwhile, endobags and clip appliers are used only in specific surgical steps, resulting in their relatively lower occurrence.

In terms of action distribution, the trend aligns with that observed in CholecT50 [6], with retract being the most dominant action. This high frequency reflects the constant need to maintain a clear surgical field during both phases, making retraction a critical and routine action. Regarding targets, the distribution similarly reflects that of CholecT50, but with expanded coverage in ProstaTD. Beyond anatomical structures, our annotations also include non-biological objects such as catheters, gauze, and endobags, which are occasionally involved in real surgical workflows. Although these targets appear less frequently, their inclusion enhances the dataset’s clinical realism and annotation diversity. Finally, due to our annotation protocol incorporating explicit triplet action boundaries with defined start and end points, a notable portion of the dataset includes triplets with null actions or targets. These annotations capture transition phases and idle tool states, elements often overlooked in other datasets, which are essential for modeling the full temporal complexity of surgical scenes.

4.3 Frequency of Triplet Occurrence

Similar to the CholecT50 [6] dataset, our ProstaTD exhibits a pronounced long-tail distribution, with many triplet categories occurring only a few times. This phenomenon is especially evident due to the dataset’s diverse sources. Variability in surgical styles contributes significantly to this distribution: different surgeons often adopt individualized preferences when switching instruments. Some may choose to continue using a currently available tool for efficiency, rather than waiting for the ideal instrument. Moreover, rare triplets may arise from patient-specific anatomical variations that necessitate atypical actions or additional procedural steps. Consequently, a large number of infrequent triplets naturally emerge in the dataset. In real surgical settings, it is neither feasible to predict

every possible instrument–action–target combination nor to exclude human error or improvisation. Capturing such variability, although challenging, is essential for building robust recognition systems. For approaches that decompose triplet prediction into separate instrument, action, and target branches, these rare triplets present valuable opportunities to evaluate model generalizability to abnormal or uncommon scenarios. This capability is particularly critical for real-world deployments, where resilience to unseen and abnormal cases significantly enhances the reliability and adaptability.

5 Evaluation

In this section, we evaluate our ProstaTD dataset with different advanced methods. Due to space limitations, we defer several detailed analyses to the supplementary materials, including confusion matrix analysis, network implementation details, extensive dataset visualizations and statistical information, limitations and future research directions, as well as discussions on the ethical statement.

5.1 Dataset Partition

Following the protocol used in RDV [6] with the CholecT50 [6] dataset, we adopt a similar strategy to partition the ProstaTD dataset into training, validation, and test sets. Specifically, we randomly selected five videos for the test set: two from our in-house PWH collection, one from the ESAD [12], and two from PSI-AVA [11]. For the validation set, we selected two videos: one from PWH and one from PSI-AVA based on the similarity in instrument appearance between the PSI-AVA and ESAD datasets. The remaining fourteen videos were allocated to the training set. Detailed statistics of the dataset partition are provided in the supplementary materials.

5.2 Metrics

We use mean Average Precision (mAP) as the primary metric to evaluate the accuracy of our model. Following previous work [6], the calculation of mAP differs for the classification task. Unlike the triplet classification where component mAP (mAP_I , mAP_V , mAP_T) are obtained by aggregating the triplet probability vectors, our detection mAP is directly computed based on the component categories. Additionally, to provide a comprehensive evaluation, we also measure the model’s computational efficiency using Frames Per Second (FPS) and conduct Precision-Recall analysis to assess the trade-off between precision and recall.

5.3 Comparison Methods

To validate the effectiveness of the proposed ProstaTD dataset, we evaluate a range of advanced methods, including both weakly supervised triplet detectors and state-of-the-art (SOTA) object detection frameworks. We first include Tripnet-Det [4] and RDV-Det [10, 6], which are detection-based adaptations of Tripnet and RDV. In the previous challenge [10], RDV relied solely on class labels for weak supervision, employing Class Activation Maps [24] and Non-Maximum Suppression for triplet localization. Following this paradigm, we implement Tripnet-Det for ProstaTD. Other challenge methods were excluded due to incomplete methodological descriptions, unavailable code, or inferior reported performance. These weakly supervised baselines are primarily included to highlight the performance gap between weak and fully supervised methods utilizing bounding box.

We further compare ProstaTD performance using state-of-the-art detection architectures. For DETR-based architectures, we use Deformable-DETR [25] and RT-DETR [26]. For YOLO-based architectures, we employ official implementations of Yolov5 [27], Yolov8 [28], and Yolov11 [29] from the Ultralytics repository. We also include comparisons with several newer versions of YOLO architectures [30–32]. In addition, we propose a baseline method named YOLO-Triplet, which integrates principles from YOLO, Tripnet [4], and RDV [6]. This two-stage framework employs YOLOv12 [32] to detect surgical instruments and their bounding boxes. Subsequently, guided by the instrument predictions, we perform cross-attention between the cropped instrument regions and an action–target recognition module based on ResNet18 [33]. Unlike Tripnet and RDV, which rely on CAMs [24] for guidance, our model uses attention-based fusion to inform the action and target branches. A decoder architecture similar to that of Tripnet is then used to infer triplet relationships. We present YOLO-Triplet as a baseline that balances inference speed and recognition accuracy. The full architecture is detailed in the supplementary materials.

Table 4: Comparison of Mean Average Precision (mAP) scores across surgical triplet detection methods. Here, “50” denotes mAP at IoU threshold 50%, and “95” denotes mAP_{50:95}. Inference speed is reported in frames per second (FPS) on a video with a spatial resolution of 640×640 pixels per frame, using an NVIDIA RTX 4090 GPU.

Method	$mAP_I(\%) \uparrow$		$mAP_V(\%) \uparrow$		$mAP_T(\%) \uparrow$		$mAP_{IVT}(\%) \uparrow$		FPS \uparrow
	50	95	50	95	50	95	50	95	
Tripnet-Det [4]	1.42	-	0.33	-	0.15	-	0.01	-	331.8
RDV-Det [10, 6]	1.73	-	0.32	-	0.15	-	0.03	-	146.6
Def-DETR [25]	68.20	59.74	43.28	38.51	34.97	31.23	21.88	19.61	67.1
RT-DETR [26]	74.62	64.45	48.17	42.96	38.63	34.26	23.64	20.79	98.0
Yolov5 [27]	66.39	57.26	40.96	36.44	32.50	28.77	20.59	18.15	185.2
Yolov8 [28]	83.16	76.41	55.62	51.46	46.69	42.85	33.36	30.75	161.6
Yolov9 [30]	81.73	75.71	54.15	50.31	47.30	44.06	32.34	30.22	187.7
Yolov10 [31]	84.17	77.12	56.61	52.16	48.86	45.20	35.05	32.39	185.7
Yolov11 [29]	82.58	75.94	55.27	51.17	48.84	45.14	34.01	31.37	188.0
Yolov12 [32]	81.79	75.47	56.23	51.99	48.00	44.82	34.08	31.79	138.3
Yolo-Triplet (Ours)	92.73	84.54	49.54	46.75	43.71	41.21	36.02	33.81	77.4

Table 5: Precision, Recall, and F_1 -score of advanced detectors on our ProstaTD test set, evaluated at the IVT component. Values are in %.

Metric	RT-DETR [26]	YOLOv10 [31]	YOLOv11 [29]	YOLOv12 [32]	YOLO-Triplet (Ours)
Precision \uparrow	41.28	35.62	33.06	35.06	35.32
Recall \uparrow	27.53	35.58	36.21	35.98	36.20
$F_1 \uparrow$	27.38	30.86	30.52	31.13	31.26

5.4 Results and Discussion

Detection Performance Analysis. As summarized in Table 4, the two weakly-supervised pipelines, Tripnet-Det [4] and RDV-Det [10, 6], yield extremely low mAP scores. This is primarily due to their reliance on class labels, which provide only weak supervision. Moreover, such supervision also fails to distinguish between co-occurring instruments and cannot reliably associate instruments with their corresponding actions and targets. In contrast, fully supervised methods exhibit a clear performance gap between DETR-based and YOLO-based architectures. With the exception of the earlier YOLOv5 [27], all YOLO variants substantially outperform Deformable DETR [25] and RT-DETR [26] both in accuracy and in speed, with YOLOv10 [31] achieving the best trade-off between detection precision and time efficiency. Our proposed *YOLO-Triplet* uses YOLO’s robust object detection backbone to attain the highest instrument-level mAP. However, its second-stage relation modeling head exhibits limited capability in capturing the complex interdependencies among instruments, actions, and targets. This results in lower performance on action and target branches and only modest improvements in the overall triplet detection metric. Additionally, the two-stage design incurs a reduction in frame rate. These results suggest that designing more expressive yet lightweight relational modules capable of modeling triplet semantics without compromising real-time performance remains a critical direction for future research.

Precision-Recall Analysis. Like other surgical triplet datasets, our ProstaTD is markedly class-imbalanced, and in a medical context both false positives and false negatives are critical. We therefore complement mAP with Precision, Recall and F_1 at IoU = 0.50 (Table 5). RT-DETR achieves the highest Precision (41.28%) but records the lowest Recall (27.53%) and F_1 (27.38%), reflecting an overly conservative strategy. YOLOv12 offers the best baseline balance (35.06% / 35.98% / 31.13%), while our YOLO-Triplet, built on the same backbone, slightly improves all three metrics to 35.32%, 36.20% and 31.26%. Although initially promising, these preliminary results remain significantly below the threshold required for reliable clinical deployment, indicating substantial scope for further exploration with our comprehensive ProstaTD dataset.

6 ProstaTD Dataset for Tracking

In this section, we introduce tracking tasks in surgical videos and their role in enhancing surgical procedures. We then present the tracking annotations in our ProstaTD dataset, emphasizing the detailed instrumentation movements and interactions captured throughout surgical workflows. Additionally, we compare the tracking annotations of ProstaTD with the Cholectrack20 dataset, highlighting the strengths and distinctive aspects of ProstaTD for surgical tracking research. Due to space constraints, we provide only a brief analysis and dataset overview here. For detailed structures and baseline experiments, please refer to our supplementary materials.

6.1 Perspective Tracking in Surgical Videos

In surgical video tracking tasks, the focus is primarily on monitoring the positions and movements of surgical instruments. This task is essential for enhancing surgical navigation and providing real-time feedback to surgeons. However, current tracking datasets often only focus on instrument tracking, rather than a comprehensive triplet tracking task that can simultaneously recognize actions and their corresponding target labels, which limits the ability to perform a comprehensive surgical assessment.

According to [17], Surgical tracking tasks are categorized into three perspectives: Intraoperative, Intracorporeal, and Visibility. Below, I will analyze the clinical and artificial intelligence significance of each perspective in major surgeries. In addition, we propose a new perspective called Triplet Perspective, which is an extension based on the Intraoperative Perspective.

Intraoperative Perspective. Current studies [34, 35] have adopted this perspective to address inventory management and skill evaluation tasks. According to our team’s clinical expertise in computer-assisted surgery, the intraoperative perspective provides the most clinically relevant framework for surgical tool tracking as it captures the complete lifecycle of each instrument from initial insertion to final removal during the procedure. This comprehensive tracking enables critical applications like real-time tool usage monitoring, procedural proficiency assessment, and surgical workflow optimization by preserving tool identity continuity despite temporary occlusions or out-of-view intervals. The intraoperative perspective’s ability to model tool replacements and reinsertions makes it indispensable for preventing retained surgical items and analyzing operator-specific instrument handling patterns. Additionally, by incorporating intraoperative track ID annotations into the surgical triplet detection task, we can better distinguish between different instances over time within the same instrument category, which is especially beneficial for complex surgical procedures.

Intracorporeal and Visibility Perspectives. The Visibility perspective focuses exclusively on tool movements within the camera’s field of view. Existing studies, such as those by [36] and [37], have utilized the Visibility perspective for real-time feedback and skill assessment. However, this perspective has limitations both macroscopically and microscopically. At the macro level, it overlaps significantly with the broader Intraoperative perspective in addressing clinical needs, as lifelong tracking inherently subsumes visibility-based trajectories, making the Visibility perspective redundant for many practical applications. The frequent changes in track IDs due to tools moving in and out of view contradict the reality that they originate from the same physical object. At the micro level, while it captures momentary visibility changes, it fails to incorporate crucial action-target interactions and cannot support detailed action assessment needs. This makes the perspective insufficient for both comprehensive surgical workflow understanding and fine-grained surgical skill evaluation.

The Intracorporeal perspective, first proposed in [17], defines instrument trajectories based on entry and exit events through trocar ports. Although this pioneering work made a valuable contribution by introducing a novel perspective on surgical instrument tracking, it overly emphasizes the physical state of "being inside the body", which heavily relies on inference. While it provides additional information regarding the frequency of instrument entry and exit events, the clinical value of this information for understanding the overall surgical procedure is somewhat limited, yet significantly increases the complexity and cost of data annotation and modeling. This limitation is particularly evident in major robotic surgeries like prostatectomy, which involves more trocar ports than laparoscopic cholecystectomy, as shown in Table 2. While these additional ports allow instruments to be temporarily placed inside without removal, a clinically safe practice, the Intracorporeal perspective’s focus on whether instruments are inside or outside the body holds limited clinical significance, as these actions are already standardized and safe. Moreover, in practice, accurately inferring the state of instruments outside the camera’s field of view is challenging and error-prone, especially in major

surgeries (such as prostatectomy) with multiple trocar ports, leading to low annotation accuracy. Therefore, we adopted the Intraoperative perspective, which has already demonstrated sufficient clinical value.

Triplet Perspective. Given the limitations of existing perspectives, particularly the Visibility perspective’s inability to capture action-target interactions and comprehensive surgical workflows, we propose a new Triplet Perspective. This perspective transcends traditional instrument-only tracking by incorporating complete surgical action units (instrument-action-target triplets). Under this perspective, a new track ID is assigned not only when instruments change but also when the action or target components of the triplet change, enabling us to capture the semantic evolution of surgical actions. Furthermore, identical triplet combinations maintain the same track ID throughout the same video, enabling both fine-grained action unit tracking and improved discrimination between multiple instances of the same type of instrument operating simultaneously. This approach addresses both macro-level surgical workflow understanding and micro-level action assessment needs, providing a more comprehensive framework for surgical analysis. While existing tracking datasets and research primarily focus on instrument-level tracking, there remains a significant research gap in developing datasets and methods that can capture this richer triplet-based tracking information, which is essential for advanced surgical skill assessment and workflow analysis.

6.2 ProstaTD Tracking Annotations Structures

Given the limitations of Intracorporeal and Visibility perspectives discussed earlier, the current tracking annotations in the ProstaTD dataset are restricted to the Intraoperative perspective and Triplet perspective track IDs. The structure of our ProstaTD tracking annotation is detailed in Table 6. As shown in the table, we annotated 21 robotic prostatectomy videos under both perspectives. The Intraoperative perspective, which tracks instruments throughout their entire surgical usage, resulted in 204 unique track IDs. In contrast, the Triplet perspective assigns different track IDs to instruments of the same category (e.g., different forceps or different needle drivers) and further generates new track IDs when the instrument-action-target composition changes. This comprehensive tracking approach generated 953 track IDs in total, reflecting both the presence of multiple instruments within the same category and the rich diversity of surgical action units captured in our dataset.

Table 6: Distribution of tracking annotations in the ProstaTD dataset. The Intraoperative perspective tracks surgical instruments throughout their complete usage duration, while the Triplet perspective tracks surgical action units based on instrument-action-target combinations and the intraoperative perspective.

Perspective	Number of Videos	Number of Track IDs
Intraoperative	21	204
Triplet	21	953

6.3 Comparison and Analysis

Since CholecTrack20 [17] was not officially released at the time of this study, we compared our ProstaTD dataset with CholecT50 [6], as CholecTrack20 shares partial video overlap with CholecT50. As shown in Table 7, ProstaTD demonstrates significantly higher instrument complexity per frame compared to CholecT50. While CholecT50 primarily contains frames with 1-2 instrument categories (38.06% and 48.72% respectively) and rarely exceeds 3 categories (2.26%), ProstaTD shows a more diverse distribution. A substantial proportion of ProstaTD frames contain 2-4 instrument categories (34.40%, 37.04%, and 15.77%), with some frames even featuring 5-6 categories (1.56% and 0.20%), highlighting the increased surgical complexity. Moreover, ProstaTD has significantly fewer frames without instruments (0.48%) compared to CholecT50 (10.97%), indicating more continuous instrument usage in robotic prostatectomy.

As illustrated in Figure 4, ProstaTD contains 165K surgical tool instances across 7 categories, with forceps (28.7%) and scissors (29.7%) being the most frequent, followed by grasper, aspirator, needle driver, clip applicator, and Endobag (Specimen bag) instruments. In contrast, CholecTrack20 [17] contains 65K instances across 7 categories, where only multiple instances of the same grasper

Table 7: Percentage distribution of instrument **categories** per frame in surgical triplet datasets between CholecT50 and ProstaTD.

Dataset	0	1	2	3	4	5	6
CholecT50 (%)	10.970	38.060	48.720	2.260	0.000	0.000	0.000
ProstaTD (%)	0.476	10.557	34.403	37.038	15.773	1.555	0.198

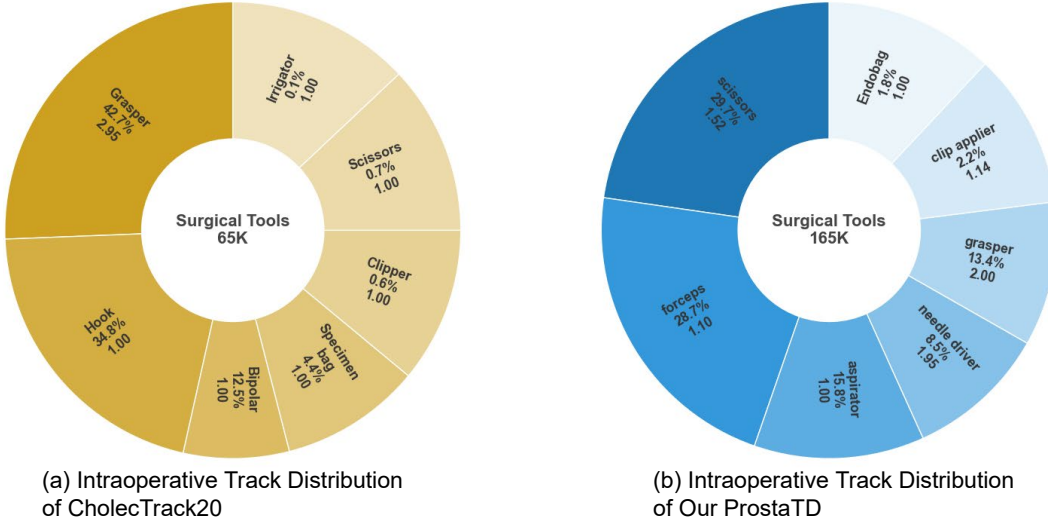


Figure 4: Distribution of surgical tool instances in CholecTrack20 (65K instances) and ProstaTD (165K instances) datasets under Intraoperative tracking perspective, where percentages indicate instrument distribution and values represent average number of tracks per video.

category appear simultaneously, making the tracking task relatively straightforward. However, in more complex major surgeries like robotic prostatectomy, multiple instances of the same category of instrument (scissors, forceps, needle driver, grasper, and clip applicator) frequently appear and operate simultaneously throughout the procedure. This is particularly evident during anastomosis, a crucial surgical phase requiring precise instrument coordination and tracking. The substantial difference in instance counts and category distribution, coupled with the frequent simultaneous use of multiple identical instruments, makes instrument tracking in ProstaTD more challenging and practically relevant for real-world major surgical applications.

7 Limitations and Future Works

Long-Tail Distribution and Rare Triplet Cases. Similar to CholecT50 [6], our ProstaTD dataset also exhibits uneven data distribution, with a significant proportion of rare triplets. These uncommon instances often arise from situational constraints, such as the time cost of instrument switching, where surgeons temporarily repurpose available tools to perform alternative actions. In addition, some triplets may be missing from the dataset due to anatomical differences between patients, which can lead to additional dissection steps or unconventional surgical techniques. In real-world procedures, the potential number of triplet combinations is far greater, influenced by variations in surgical habits, patient conditions, and even occasional errors. However, these rare and abnormal cases are difficult to capture due to their infrequent occurrence. Despite their low frequency, they are highly relevant to clinical safety and robustness, making their inclusion vital in medical datasets. Moreover, most current approaches constrain triplet recognition to a fixed predefined class set, which inherently prevents the identification of unseen or abnormal triplets. This limitation underscores the need for models that independently predict instruments, actions, and targets, and then flexibly compose triplet candidates, rather than relying on rigid class enumeration. Therefore, our ProstaTD dataset provides a venue to address this challenge, facilitating future research in surgical action recognition.

Temporal Modeling. Effectively leveraging temporal information remains a key challenge in surgical video detection. A primary limitation is the trade-off between temporal modeling and computational efficiency: incorporating temporal features often leads to increased inference cost, which is critical in real-time or resource-constrained settings. Another challenge arises from the distinctive nature of surgical videos compared to natural video domains. In surgery, many actions share similar spatial and temporal characteristics, making fine-grained differentiation inherently difficult. For example, both dissect and cut involve tissue removal; however, dissect emphasizes structural separation and exposure, whereas cut typically implies incision. These nuances reflect that certain surgical actions are defined more by intent and clinical purpose than by observable motion patterns. Future research should explore lightweight temporal modeling approaches that preserve computational efficiency while capturing essential temporal cues. Additionally, moving beyond purely spatial-temporal representations to incorporate intent-driven action semantics may enable more accurate and clinically meaningful recognition of surgical activities.

8 Broader Impacts

Positive Impact. As a comprehensive dataset for precise bounding box annotations and multi-institutional data, ProstaTD has the potential to significantly advance surgical AI development. The fine-grained annotations enable AI systems to monitor instrument-tissue interactions in real-time, generating objective skill assessments for residents and providing data-driven feedback for continuous surgical quality improvement. Our open-source, multi-center dataset significantly reduces single-source bias and promotes model generalization across different hospitals and surgical settings, establishing a new standard for surgical AI validation. This dataset empowers surgical robot manufacturers to pre-train their vision modules directly, potentially accelerating clinical translation and reducing development cycles by months or even years. Moreover, the comprehensive nature of ProstaTD could catalyze breakthrough innovations in surgical automation and safety systems, ultimately contributing to more standardized and safer surgical procedures worldwide.

Potential Risks. The dataset might be exploited by unregulated third parties for commercial products, where model failures could directly compromise patient safety. *Mitigation Measures:* (1) We implement CC-BY-NC-SA-4.0 license requiring all derivatives to maintain non-commercial terms; (2) We recommend incorporating uncertainty estimation and human oversight prompts when deploying models. (3) We explicitly prohibit unauthorized use of the dataset for training LLMs or commercial AI systems, and reserve the right to take legal action against any violations of these terms.

9 Ethical Statement

All procedures performed in this study with human participants were in accordance with ethical standards and approved by the Institutional Review Board (IRB) of Prince of Wales Hospital in Hong Kong. Informed consent was obtained from all individual participants involved in the study. All employed students were fairly compensated according to institutional guidelines and contractual agreements. To protect patient privacy and confidentiality, all surgical videos underwent specialized processing to remove any identifying information. All collected data was thoroughly anonymized and stored in secure facilities with restricted access limited to authorized research team members. The study adhered to all relevant data protection regulations and medical research guidelines throughout data collection, processing, and analysis phases.

10 Conclusion

We present ProstaTD, a large-scale surgical dataset featuring precise bounding box annotations and standardized temporal definitions across 89 triplet categories and 165,567 instances from three distinct data sources. Unlike existing datasets that rely on weak supervision, ProstaTD’s comprehensive annotations enable improved triplet detection, especially in complex multi-instrument scenarios. The dataset’s precise spatial-temporal annotations enhance model interpretability and evaluation fairness, promoting the development of more robust surgical detection frameworks. We believe ProstaTD lays a strong foundation for fine-grained surgical video understanding and opens new avenues for intelligent surgical assistance in high-complexity clinical domains.

References

- [1] A. Murali, D. Alapatt, P. Mascagni, A. Vardazaryan, A. Garcia, N. Okamoto, D. Mutter, and N. Padoy, "Latent graph representations for critical view of safety assessment," *IEEE Transactions on Medical Imaging*, pp. 1–1, 2023.
- [2] N. Padoy, T. Blum, S.-A. Ahmadi, H. Feussner, M.-O. Berger, and N. Navab, "Statistical modeling and recognition of surgical workflow," *Medical image analysis*, vol. 16, no. 3, pp. 632–641, 2012.
- [3] R. E. Harari, R. D. Dias, L. R. Kennedy-Metz, G. Varni, M. Gombolay, S. Yule, E. Salas, and M. A. Zenati, "Deep learning analysis of surgical video recordings to assess nontechnical skills," *JAMA Network Open*, vol. 7, no. 7, pp. e2422520–e2422520, 2024.
- [4] C. I. Nwoye, C. Gonzalez, T. Yu, P. Mascagni, D. Mutter, J. Marescaux, and N. Padoy, "Recognition of instrument-tissue interactions in endoscopic videos via action triplets," in *International Conference on Medical Image Computing and Computer-Assisted Intervention (MICCAI)*. Springer, 2020, pp. 364–374.
- [5] C. I. Nwoye, D. Alapatt, C. Vardazaryan, Armine ... Gonzalez, and N. Padoy, "Cholectriplet2021: a benchmark challenge for surgical action triplet recognition," *arXiv preprint arXiv:2204.04746*, 2022.
- [6] C. I. Nwoye, T. Yu, C. Gonzalez, B. Seeliger, P. Mascagni, D. Mutter, J. Marescaux, and N. Padoy, "Rendezvous: Attention mechanisms for the recognition of surgical action triplets in endoscopic videos," *Medical Image Analysis*, vol. 78, p. 102433, 2022.
- [7] N. Xi, J. Meng, and J. Yuan, "Forest graph convolutional network for surgical action triplet recognition in endoscopic videos," *IEEE Transactions on Circuits and Systems for Video Technology*, vol. 32, no. 12, pp. 8550–8561, 2022.
- [8] Y. Chen, S. He, Y. Jin, and J. Qin, "Surgical activity triplet recognition via triplet disentanglement," in *International Conference on Medical Image Computing and Computer-Assisted Intervention*. Springer, 2023, pp. 451–461.
- [9] S. Gui and Z. Wang, "Tail-Enhanced Representation Learning for Surgical Triplet Recognition," in *proceedings of Medical Image Computing and Computer Assisted Intervention – MICCAI 2024*, vol. LNCS 15011. Springer Nature Switzerland, October 2024.
- [10] C. I. Nwoye, T. Yu, S. Sharma, A. Murali, D. Alapatt, C. Vardazaryan, Armine ... Gonzalez, and N. Padoy, "Cholectriplet2022: Show me a tool and tell me the triplet: an endoscopic vision challenge for surgical action triplet detection." *arXiv preprint arXiv:2204.14746*, 2023.
- [11] N. Valderrama, P. Ruiz, I. Hernández, N. Ayobi, M. Verlyck, J. Santander, J. Caicedo, N. Fernández, and P. Arbeláez, "Towards holistic surgical scene understanding," in *Medical Image Computing and Computer Assisted Intervention – MICCAI 2022*. Cham: Springer Nature Switzerland, 2022, pp. 442–452.
- [12] V. S. Bawa, G. Singh, F. KapingA, I. Skarga-Bandurova, E. Oleari, A. Leporini, C. Landolfo, P. Zhao, X. Xiang, G. Luo *et al.*, "The saras endoscopic surgeon action detection (esad) dataset: Challenges and methods," *arXiv preprint arXiv:2104.03178*, 2021.
- [13] N. Ayobi, S. Rodríguez, A. Pérez, I. Hernández, N. Aparicio, E. Dessevres, S. Peña, J. Santander, J. I. Caicedo, N. Fernández, and P. Arbeláez, "Pixel-wise recognition for holistic surgical scene understanding," *arXiv*, 2024. [Online]. Available: <https://arxiv.org/abs/2401.11174>
- [14] N. Ayobi, A. Pérez-Rondón, S. Rodríguez, and P. Arbeláez, "Matis: Masked-attention transformers for surgical instrument segmentation," in *2023 IEEE 20th International Symposium on Biomedical Imaging (ISBI)*, 2023, pp. 1–5.
- [15] D. Psychogyios, E. Colleoni, B. Van Amsterdam, C.-Y. Li, S.-Y. Huang, Y. Li, F. Jia, B. Zou, G. Wang, Y. Liu *et al.*, "Sar-rarp50: Segmentation of surgical instrumentation and action recognition on robot-assisted radical prostatectomy challenge," *arXiv preprint arXiv:2401.00496*, 2023.

- [16] P. Shi, Z. Zhao, S. Hu, and F. Chang, “Real-time surgical tool detection in minimally invasive surgery based on attention-guided convolutional neural network,” *IEEE Access*, vol. 8, pp. 228 853–228 862, 2020.
- [17] C. I. Nwoye, F. Zaid, J. Lavanchy, and N. Padoy, “Choelectrack20: A multi-perspective tracking dataset for surgical tools,” in *IEEE/CVF Conference on Computer Vision and Pattern Recognition, Wed June 11th-Sun June 15th, 2025*, 2025.
- [18] W. Lin, Y. Hu, H. Fu, M. Yang, C.-B. Chng, R. Kawasaki, C. Chui, and J. Liu, “Instrument-tissue interaction detection framework for surgical video understanding,” *IEEE Transactions on Medical Imaging*, 2024.
- [19] A. Huauilmé, D. Sarikaya, K. Le Mut, F. Despinoy, Y. Long, Q. Dou, C.-B. Chng, W. Lin, S. Kondo, L. Bravo-Sánchez *et al.*, “Micro-surgical anastomose workflow recognition challenge report,” *Computer Methods and Programs in Biomedicine*, vol. 212, p. 106452, 2021.
- [20] S. Zhao, Y. Liu, Q. Wang, D. Sun, R. Liu, and S. K. Zhou, “Murphy: Relations matter in surgical workflow analysis,” *arXiv preprint arXiv:2212.12719*, 2022.
- [21] W. Lin, Y. Hu, L. Hao, D. Zhou, M. Yang, H. Fu, C. Chui, and J. Liu, “Instrument-tissue interaction quintuple detection in surgery videos,” in *International Conference on Medical Image Computing and Computer-Assisted Intervention*. Springer, 2022, pp. 399–409.
- [22] W. Lin, Y. Hu, H. Fu, M. Yang, C.-B. Chng, R. Kawasaki, C. Chui, and J. Liu, “Instrument-tissue interaction detection framework for surgical video understanding,” *IEEE Transactions on Medical Imaging*, 2024.
- [23] A. P. Twinanda, S. Shehata, D. Mutter, J. Marescaux, M. De Mathelin, and N. Padoy, “Endonet: a deep architecture for recognition tasks on laparoscopic videos,” *IEEE transactions on medical imaging*, vol. 36, no. 1, pp. 86–97, 2016.
- [24] B. Zhou, A. Khosla, A. Lapedriza, A. Oliva, and A. Torralba, “Learning deep features for discriminative localization,” in *Proceedings of the IEEE conference on computer vision and pattern recognition*, 2016, pp. 2921–2929.
- [25] X. Zhu, W. Su, L. Lu, B. Li, X. Wang, and J. Dai, “Deformable detr: Deformable transformers for end-to-end object detection,” *arXiv preprint arXiv:2010.04159*, 2020.
- [26] Y. Zhao, W. Lv, S. Xu, J. Wei, G. Wang, Q. Dang, Y. Liu, and J. Chen, “Detrs beat yolos on real-time object detection,” in *Proceedings of the IEEE/CVF conference on computer vision and pattern recognition*, 2024, pp. 16 965–16 974.
- [27] G. Jocher, “Ultralytics yolov5,” 2020. [Online]. Available: <https://github.com/ultralytics/yolov5>
- [28] R. Varghese and M. Sambath, “Yolov8: A novel object detection algorithm with enhanced performance and robustness,” in *2024 International Conference on Advances in Data Engineering and Intelligent Computing Systems (ADICS)*. IEEE, 2024, pp. 1–6.
- [29] R. Khanam and M. Hussain, “Yolov11: An overview of the key architectural enhancements,” *arXiv preprint arXiv:2410.17725*, 2024.
- [30] C.-Y. Wang, I.-H. Yeh, and H.-Y. Mark Liao, “Yolov9: Learning what you want to learn using programmable gradient information,” in *European conference on computer vision*. Springer, 2024, pp. 1–21.
- [31] A. Wang, H. Chen, L. Liu, K. Chen, Z. Lin, J. Han *et al.*, “Yolov10: Real-time end-to-end object detection,” *Advances in Neural Information Processing Systems*, vol. 37, pp. 107 984–108 011, 2024.
- [32] Y. Tian, Q. Ye, and D. Doermann, “Yolov12: Attention-centric real-time object detectors,” *arXiv preprint arXiv:2502.12524*, 2025.
- [33] K. He, X. Zhang, S. Ren, and J. Sun, “Deep residual learning for image recognition,” in *Proceedings of the IEEE conference on computer vision and pattern recognition*, 2016, pp. 770–778.

- [34] M. Fathollahi, M. H. Sarhan, R. Pena, L. DiMonte, A. Gupta, A. Ataliwala, and J. Barker, "Video-based surgical skills assessment using long term tool tracking," in *International Conference on Medical Image Computing and Computer-Assisted Intervention*. Springer, 2022, pp. 541–550.
- [35] C. I. Nwoye, D. Mutter, J. Marescaux, and N. Padoy, "Weakly supervised convolutional lstm approach for tool tracking in laparoscopic videos," *International journal of computer assisted radiology and surgery*, vol. 14, pp. 1059–1067, 2019.
- [36] J. L. Lavanchy, J. Zindel, K. Kirtac, I. Twick, E. Hosgor, D. Candinas, and G. Beldi, "Automation of surgical skill assessment using a three-stage machine learning algorithm," *Scientific reports*, vol. 11, no. 1, p. 5197, 2021.
- [37] M. Robu, A. Kadkhodamohammadi, I. Luengo, and D. Stoyanov, "Towards real-time multiple surgical tool tracking," *Computer Methods in Biomechanics and Biomedical Engineering: Imaging & Visualization*, vol. 9, no. 3, pp. 279–285, 2021.